ChemComm

COMMUNICATION

View Article Online
View Journal

Check for updates

Cite this: DOI: 10.1039/c9cc06492c

Received 21st August 2019,
Accepted 10th November 2019

DOI: 10.1039/c9cc06492c

rsc.li/chemcomm

Through-space π-delocalization in a conjugated macrocycle consisting of [2.2]paracyclophane†

Yayu Wu,[a] Guilin Zhuang,*[b] Shengsheng Cui,[a] Yu Zhou,[a] Jinyi Wang,[a] Qiang Huang[a] and Pingwu Du*[a]

Herein, we report the synthesis and characterization of a [2.2]paracyclophane-containing macrocycle (PCMC) as a new through-space conjugated macrocycle using only benzene groups as the skeleton. For comparison, a diphenylmethane-containing nanohoop macrocycle (DCMC) with a non-conjugated linker was also synthesized. Their structures were confirmed by NMR and HR-MS, and their photophysical properties were studied by UV-vis and fluorescence spectroscopies combined with theoretical calculations. The strain energy of PCMC was estimated to be as high as 72.58 kcal mol^{-1}.

Conjugated macrocycles have received much attention due to their unique cyclic structures, intrinsic photoelectric properties, and extensive material application prospects.[1–4] Research on conjugated macrocycles started in the early 1960s,[5] and great progress has been made in the last two decades.[3,6] To date, a series of conjugated macrocycles consisting of thiophene, benzene, pyridine, and acetylene units have been widely studied.[7–12] Inspired by these studies, large π-extended nanographene units (such as hexa-*peri*-hexabenzocoronene, HBC) have been successfully introduced into hoop-shaped macrocycle backbones.[13,14] Conjugated macrocycles have many interesting advantages as organic materials, such as altered electronic structures,[11,15] no end groups to create defects as trap-sites,[16,17] and a tunable cavity to host guest molecules.[14,18] However, most conjugated macrocycles usually consist of sp^2 carbon skeletons, and through-space conjugated macrocycles consisting of π-stacked systems have been studied only rarely despite their importance in optoelectronic applications.[19,20]

[2.2]Paracyclophane is an appealing aromatic compound including face-to-face benzene rings ("decks") fixed by two ethylene chains ("bridges") with a deck distance of approximately 3.0 Å.[21,22] The slightly bent but stable structure of [2.2]paracyclophane enables through-space electronic communication between the benzene decks.[23] Moreover, [2.2]paracyclophane can be introduced as a chiral scaffold providing target compounds with interesting chiral properties.[24,25] Naturally, the introduction of [2.2]paracyclophane as a building block into conjugated macrocycles can realize the construction of π-stacked systems in the cyclic structure.[26] In 2001, Haley, Boydston, and coworkers successfully obtained an open-circuited conjugated macrocycle containing [2.2]paracyclophane and dehydrobenzoannulene units,[27] which demonstrated "global" through-space delocalization between the conjugated decks of the annelated cyclophanes. Casado and coworkers synthesized a series of stilbenoid and thiophenic compounds containing [2.2]paracyclophane units, and then studied their photophysical properties regarding the effect of through-bond and through space π-electron delocalization.[28] Recently, Ogoshi and coworkers reported through-space π-delocalization properties in a pillar[5]arene.[29] However, studies on through-space π-conjugated benzene-based macrocycles are relatively rare, and the synthesis of such macrocycles remains challenging.

In this present study, we report the synthesis of a conjugated [2.2]paracyclophane-containing macrocycle (**PCMC**) (Fig. 1),

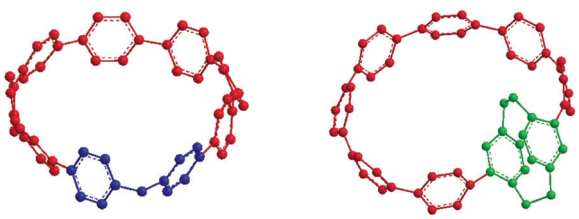

Fig. 1 DFT optimized geometries of the designed macrocycles **DCMC** and **PCMC**.

[a] Hefei National Laboratory of Physical Science at the Microscale, CAS Key Laboratory of Materials for Energy Conversion, Department of Materials Science and Engineering, iChEM (Collaborative Innovation Center of Chemistry for Energy Materials), University of Science and Technology of China, 96 Jinzhai Road, Hefei, Anhui Province, 230026, China. E-mail: dupingwu@ustc.edu.cn; Fax: +86-551-63606207; Tel: +86-551-63606207

[b] College of Chemical Engineering, Zhejiang University of Technology, 18 Chaowang Road, Hangzhou, Zhejiang Province, 310032, China. E-mail: glzhuang@zjut.edu.cn; Fax: +86-571-88871037; Tel: +86-571-88871037

† Electronic supplementary information (ESI) available. See DOI: 10.1039/c9cc06492c

which represents the first through-space conjugated macrocycle composed of benzene rings. **PCMC** should have two enantiomers (PCMC-S0 and PCMC-S1, Fig. S1, ESI†) and changes into a mirror image by rotating around single bonds at room temperature without experiencing a flat achiral conformation process.[30] Meanwhile, a transition state (PCMC-TS) was also obtained with the rotation-energy barrier of 30.72 kJ mol^{-1} above PCMC-S0. For comparison, a diphenylmethane-containing macrocycle (**DCMC**) with similar size and twist angles was also synthesized and characterized.[31,32] These macrocycles were studied by high-resolution mass spectrometry (HR-MS), ^{1}H, ^{13}C and 2D nuclear magnetic resonance (NMR) spectroscopies, steady-state spectroscopies, time-resolved photoluminescence decay, and theoretical calculations.

Our strategy for the synthesis of **DCMC** and **PCMC** is to connect the C-shaped fragment **1**, a suitably curved synthon, with compounds **2** and **3**, respectively. Then, the target product can be obtained by subsequent aromatization reactions. As shown in Fig. 2, the C-shaped synthon **1** was facilely synthesized on a gram scale starting from 4′-bromo-[1,1′-biphenyl]-4-ol over two steps with high yields (>50%) according to a recently reported method.[17,33] To construct the through-space π-conjugated macrocycle **PCMC**, 4,16-diboryl [2.2]paracyclophane **3** was synthesized (yield > 70%) from 4,16-dibromo[2.2]paracyclophane using $Pd(dppf)Cl_2$ as the catalyst in DMF. Moreover, bis(4-borylphenyl)methane **2** was synthesized according to a reported method[31] to construct a diphenylmethane-containing macrocycle **DCMC**. Finally, the target nanohoop macrocycles **DCMC** and **PCMC** were prepared by Suzuki coupling reactions between the synthon **1** and the pinacol boronic ester **2** or **3** using $Pd(PPh_3)_4$ as the catalyst at 75 °C, followed by reductive aromatization reactions using sodium naphthalide at −78 °C.

The successful synthesis of **DCMC** and **PCMC** can be confirmed by HR-MS and NMR spectroscopies (Fig. 3 and Fig. S2–S12, ESI†). The exact mass spectrometries show the main peaks at *m*/*z* 698.2980 for **DCMC** and 738.3257 for **PCMC**, which match well

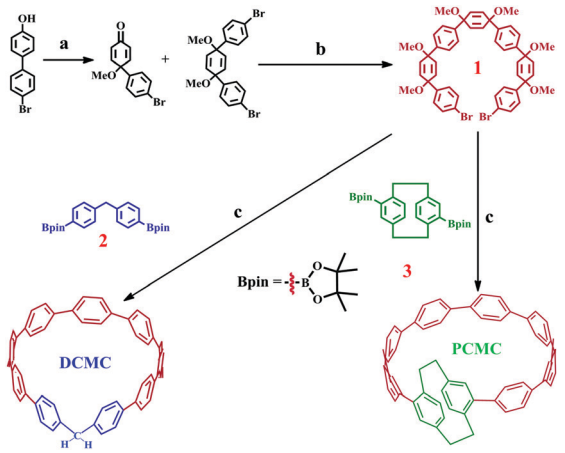

Fig. 2 Synthetic procedure for the macrocycles **DCMC** and **PCMC**. Reaction conditions: (a) DAIB, MeOH, RT, 48 h; (b) (1) *N*-BuLi, THF, −78 °C, 2 h; (2) NaH, MeI, THF, 0 °C, 8 h; (c) (1) KOH, $Pd(PPh_3)_4$, THF/H_2O, 75 °C, 48 h; (2) Sodium naphthalide/THF, −78 °C, 2 h.

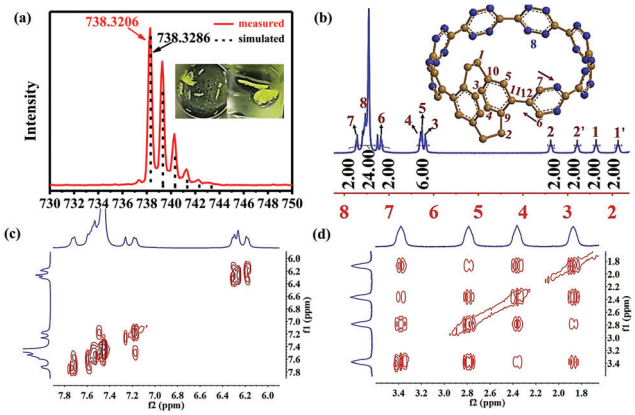

Fig. 3 (a) HR-MS (MALDI-TOF) spectrometry for **PCMC**. Insert: tiny crystal photographs of **PCMC**. (b) ^{1}H NMR spectrum for **PCMC**. ^{1}H–^{1}H COSY NMR spectra of the aromatic protons (c) and alkane protons (d) for **PCMC**.

with the simulated mass data (698.2973 for **DCMC** and 738.3286 for **PCMC**). Through slow solvent evaporation (v/v, methanol/CH_2Cl_2 = 4 : 1), we obtained yellow needle-like crystals of **PCMC**, but failed to collect useful X-ray diffraction data so far (Fig. 3a, inset). The ^{1}H NMR spectrum of **PCMC** in $CDCl_3$ is shown in Fig. 3b. The aromatic protons of **PCMC** appear in the region of 6.09–7.71 ppm, and the multiplets at 7.65–7.30 ppm (H_8) can be assigned to the protons in the C-shaped *para*-linked benzene fragment according to the position and integrated areas of the ^{1}H NMR peaks. Due to the difference between the inner and outer ring shielding effects, the resonances at δ = 7.71 and 7.18 ppm can be assigned to the H_7 and H_6 atoms, respectively. Since the 2D ^{1}H–^{1}H COSY NMR data have no obvious cross peaks between the multiplets at 7.65–7.30 and 6.37–6.09 ppm (Fig. 3c), the signals at 6.37–6.09 ppm are tentatively assigned to the protons in the [2.2]paracyclophane unit. To further assign the NMR resonances for **PCMC**, we carried out DEPT, HMBC, and HSQC measurements (Fig. S6–S10, ESI†). Based on these 2D-NMR spectra, most of the observed signals in ^{1}H- and ^{13}C-NMR for **PCMC** (Fig. S11 and S12, ESI†) can be assigned. Notably, the bridged methylenes of the cyclophane unit in **PCMC** have four separated resonances in the region of 1.80–3.40 ppm which shifted to a higher field than the proton signals of the methylene unit in **DCMC** and show significant cross peaks between each other (Fig. 3d), which can be ascribed to the through-space communication and cyclic structure of **PCMC**. This through-space π-delocalization was further confirmed by the 2D NOESY and ROESY NMR spectra (Fig. S13, ESI†), which revealed the close spatial relationship of protons on four methylene groups.

The photophysical properties of **DCMC** and **PCMC** were further studied by UV-vis absorption and fluorescence spectroscopies at room temperature in the air atmosphere (Fig. 4a). The diluted solution of **DCMC** in CH_2Cl_2 ($c = 1.0 \times 10^{-5}$ M) displayed obvious absorption bands in the range of 250–450 nm, and maximized at 323 nm ($\varepsilon = 4.32 \times 10^{4}$ M^{-1} cm^{-1}) along with a small shoulder at 380 nm ($\varepsilon = 0.89 \times 10^{4}$ M^{-1} cm^{-1}). In contrast, the absorption band of **PCMC** is redshifted, demonstrating an absorption maximum at 326 nm along with one shoulder peak

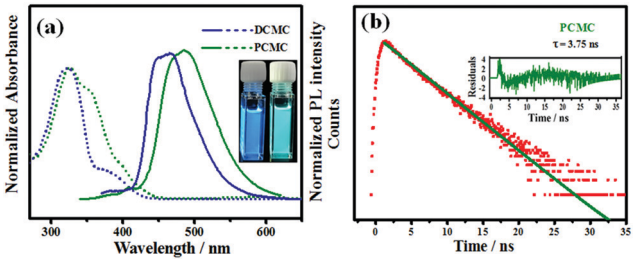

Fig. 4 (a) UV-vis absorption (dashed lines) and fluorescence spectra (solid lines) for **DCMC** (blue) and **PCMC** (red) in CH_2Cl_2 (1.0×10^{-5} M). Inset: Fluorescence photographs of **DCMC** (left) and **PCMC** (right) in CH_2Cl_2 under UV irradiation at λ = 365 nm. (b) Fluorescence decay lifetime for **PCMC** in CH_2Cl_2 measured at λ = 488 nm. Insert: Curve-fitting residuals for **PCMC**.

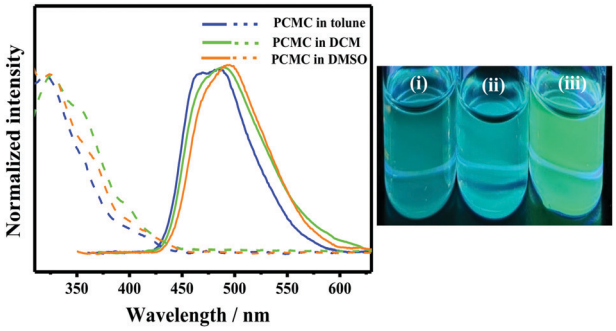

Fig. 5 (left) UV-vis absorption (dashed lines) and fluorescence spectra (solid lines) for **PCMC** in different solvents (1.0×10^{-5} M). (Right) Fluorescence photographs of **PCMC** in different solvents (i: toluene; ii: DCM; iii: DMSO.) under UV irradiation at λ = 365 nm.

at 355 nm and one small shoulder peak at 398 nm. The molecular absorption coefficients for these absorption peaks are 2.89×10^4, 2.10×10^4, and 0.54×10^4 M^{-1} cm^{-1}, respectively. Compared with the absorption feature of **DCMC**, the redshift and extended absorption of **PCMC** can also be ascribed to the π-stacked structure of the cyclophane moiety undergoing through-space interaction.[34,35]

The fluorescence emission spectrum of **DCMC** exhibited one vibronic emission band maximized at 458 nm upon excitation at 320 nm. Interestingly, the emission spectrum of **PCMC** showed an apparent redshift feature with one maximum emission peak at 488 nm. Compared to the Stokes shift of **DCMC**, **PCMC** has a larger Stokes shift of 27 nm, probably due to the π-stacked through-space conjugation and/or the increased flexibility of **PCMC**.[29] Using anthracene as the reference (Φ_F = 30% in ethanol), the photoluminescence quantum yields of **DCMC** and **PCMC** were determined to be Φ_F = 37% and Φ_F = 31%, respectively. Under a hand-held UV lamp excited at λ = 365 nm, the photoluminescence of **PCMC** in a solid and in CH_2Cl_2 solution ($c = 1.0 \times 10^{-5}$ M) presents an intense green color, whereas **DCMC** is blue (Fig. 4a, inset and Fig. S15a, ESI†).

A time-resolved photoluminescence (TRPL) technique was carried out to investigate the excited-state lifetimes of **DCMC** and **PCMC** in CH_2Cl_2 at room temperature. The PL decay results of **DCMC** and **PCMC** are shown in Fig. S15b (ESI†) and Fig. 4b. Upon excitation at 320 nm, the luminescence lifetime of **PCMC** was determined to be approximately 3.75 ns at 488 nm by single-exponential decay fitting. The curve fitting residuals confirm the accuracy of the TRPL measurement results (Fig. S15b (ESI†) and Fig. 4b, inset). As for **DCMC**, a single-exponential decay was observed with one lifetime of 2.95 ns at 458 nm when excited at 320 nm. These different photophysical data also indicate the structural discrepancy between **DCMC** and **PCMC**.

Through-space π-delocalization in a conjugated system is sensitive to the polarity of solvents.[36] Table S1 (ESI†) summarizes the spectral data for **PCMC** and **DCMC** in different solvents from hexane (a nonpolar solvent) to dimethyl sulfoxide (a polar solvent). As shown in Fig. 5 and Table S1 (ESI†), the UV-vis absorption of **PCMC** is only slightly affected by the solvent polarity,[37] indicating that the ground state of **PCMC** has no significant intramolecular charge transfer (ICT) character compared to **DCMC**.[38–40] However, the emission features of **PCMC** show obvious changes in different solvents, as evidenced by a color change from green to yellow with increasing solvent polarities (Fig. 5, inset). The PL maximum peak of **DCMC** in DMSO is only slightly red shifted by ~7 nm (0.04 eV) compared to that in toluene. In contrast, the PL maximum peak of **PCMC** in DMSO is redshifted up to ~38 nm (0.21 eV).[41,42] We propose that through-space π-delocalization across the [2.2]para-cyclophane core is more polarizable than through-bond interaction in the excited state.[43,44]

To investigate the dynamic racemization process of **PCMC**, we performed VT-NMR experiments in CD_2Cl_2. When the temperature was decreased from 273 K to 198 K, the methylene proton resonances in the cyclophane unit showed appreciable changes of the chemical shifts, indicating its interesting racemization behavior (Fig. S16, ESI†). At 273 K, the methylenes have four singlets in the range of 1.4–4.1 ppm, demonstrating that the ring rotation process is rapid on the NMR time scale.[45] As the temperature decreases, the rotation process should slow down, and the spectrum will have more resonances if **PCMC** is conformationally rigid. At ~198 K, the proton resonances in 1.4–3.0 ppm show obvious line broadening and were split into small peaks with partially overlapping signals (Fig. S16, ESI†), confirming the dynamic racemization process of **PCMC** using the rubber glove mechanism.[25] The activation barrier for the racemization of **PCMC** was estimated to be 36 kJ mol^{-1} based on the shift difference of 198 Hz for $H_1/H_{1'}$ and the coalescence temperature (198 K).[46]

Variable-temperature UV-vis and fluorescence spectra were further recorded. By increasing the temperature (Fig. S17a, ESI†), the absorption intensity of **PCMC** in THF decreased, which is probably due to the faster rotational motions at a higher temperature to reduce effective electronic transitions.[47] Notably, the fluorescence spectra of **PCMC** in the solid state exhibited an interesting change when the temperature was increased from 50 K to 300 K (Fig. S17b, ESI†). The single broad emission band was split into two peaks with a substantial increase of the emission intensity when decreasing the temperature below 250 K. Furthermore, the results showed that **PCMC** gradually becomes conformationally rigid at temperatures below 250 K (Fig. S16, ESI†). The increase of molecular rigidity can reduce the quenching rate of the excited state and increase the coplanarity

of **PCMC**, further enhancing the through-space π-delocalization effect.[48] As a result, the low temperature can reduce the flexibility of the macrocycle and facilitate the through-space π-delocalization, resulting in enhanced absorption and emission intensities.[49]

In order to further reveal the molecular geometry and electronic nature of these two macrocycles, we performed density functional theory calculations at the theoretical level of B3LYP/Def2-TZVP using the Gaussian 09 software.[50] The strain energy is calculated to be 46.22 kcal mol^{-1} for **DCMC** and the HOMO–LUMO gap is 3.42 eV for **PCMC** and 3.31 eV for **DCMC**. All the results can be found in Fig. S18–S22 (ESI†).

In conclusion, we have successfully synthesized a through-space π-delocalization conjugated macrocycle (**PCMC**) using palladium-catalyzed Suzuki–Miyaura coupling followed by the reductive aromatization reaction. Compared to a diphenylmethane-containing conjugated macrocycle (**DCMC**), **PCMC** showed noticeable redshifts in both absorption and emission spectra owing to its π-stacked structure with through-space interaction. In addition, the solvent effect of **PCMC** confirms the solvatochromism of the through-space charge transfer in the cyclic conjugated system. Furthermore, challenges in terms of synthesizing large π-extended through-space conjugated macrocycles and developing their practical optoelectronic applications are the subjects of ongoing work in our laboratory.

This work was financially supported by the National Key Research and Development Program of China (2017YFA0402800), the National Natural Science Foundation of China (21971229 and 51772285), the National Synchrotron Radiation Laboratory at USTC, and the Zhejiang Provincial Natural Science Foundation (No. LR19B010001).

Conflicts of interest

There are no conflicts to declare.

Notes and references

1 C. Grave and A. D. Schlüter, *Eur. J. Org. Chem.*, 2002, 3075–3098.
2 J. Casado, V. Hernández, R. Ponce Ortiz, M. C. Ruiz Delgado, J. T. López Navarrete, G. Fuhrmann and P. Bäuerle, *J. Raman Spectrosc.*, 2004, **35**, 592–599.
3 W. Zhang and J. S. Moore, *Angew. Chem., Int. Ed.*, 2006, **45**, 4416–4439.
4 Z. Liu, S. K. M. Nalluri and J. F. Stoddart, *Chem. Soc. Rev.*, 2017, **46**, 2459–2478.
5 F. Sondheimer, *Pure Appl. Chem.*, 1963, **7**, 363–388.
6 T. Kawase and H. Kurata, *Chem. Rev.*, 2006, **106**, 5250–5273.
7 F. Zhang and P. Bäuerle, *J. Am. Chem. Soc.*, 2007, **129**, 3090–3091.
8 J. Sreedhar Reddy and V. G. Anand, *Chem. Commun.*, 2008, 1326–1328.
9 R. Jasti, J. Bhattacharjee, J. B. Neaton and C. R. Bertozzi, *J. Am. Chem. Soc.*, 2008, **130**, 17646–17647.
10 B. Farajidizaji, C. Huang, H. Thakellapalli, S. Li, N. G. Akhmedov, B. V. Popp, J. L. Petersen and K. K. Wang, *J. Org. Chem.*, 2017, **82**, 4458–4464.
11 F. Lucas, L. Sicard, O. Jeannin, J. Rault-Berthelot, E. Jacques, C. Quinton and C. Poriel, *Chem. – Eur. J.*, 2019, **25**, 7740–7748.
12 D. Wassy, M. Pfeifer and B. Esser, *J. Org. Chem.*, 2019, DOI: 10.1021/acs.joc.9b01195.
13 D. Lu, H. Wu, Y. Dai, H. Shi, X. Shao, S. Yang, J. Yang and P. W. Du, *Chem. Commun.*, 2016, **52**, 7164–7167.
14 D. P. Lu, G. L. Zhuang, H. T. Wu, S. Wang, S. F. Yang and P. W. Du, *Angew. Chem., Int. Ed.*, 2017, **56**, 158–162.
15 J. Krömer, I. Rios-Carreras, G. Fuhrmann, C. Musch, M. Wunderlin, T. Debaerdemaeker, E. Mena-Osteritz and P. Bäuerle, *Angew. Chem., Int. Ed.*, 2000, **39**, 3481–3486.
16 A. C. Arias, J. D. MacKenzie, I. McCulloch, J. Rivnay and A. Salleo, *Chem. Rev.*, 2010, **110**, 3–24.
17 Z. He, X. Xu, X. Zheng, T. Ming and Q. Miao, *Chem. Sci.*, 2013, **4**, 4525–4531.
18 T. Kawase, K. Tanaka, Y. Seirai, N. Shiono and M. Oda, *Angew. Chem., Int. Ed.*, 2003, **42**, 5597–5600.
19 H. C. Lin, W. Y. Lin, H. T. Bai, J. H. Chen, B. Y. Jin and T. Y. Luh, *Angew. Chem., Int. Ed.*, 2007, **46**, 897–900.
20 E. Elacqua and L. R. MacGillivray, *Eur. J. Org. Chem.*, 2010, 6883–6894.
21 I. Majerz and T. Dziembowska, *J. Phys. Chem. A*, 2016, **120**, 8138–8147.
22 E. Spuling, N. Sharma, I. D. W. Samuel, E. Zysman-Colman and S. Brase, *Chem. Commun.*, 2018, **54**, 9278–9281.
23 Y. Morisaki and Y. Chujo, *Polym. Chem.*, 2011, **2**, 1249–1257.
24 M. Hasegawa, K. Kobayakawa, H. Matsuzawa, T. Nishinaga, T. Hirose, K. Sako and Y. Mazaki, *Chem. – Eur. J.*, 2017, **23**, 3267–3271.
25 K. J. Weiland, T. Brandl, K. Atz, A. Prescimone, D. Haussinger, T. Solomek and M. Mayor, *J. Am. Chem. Soc.*, 2019, **141**, 2104–2110.
26 C.-Y. Yu and Y.-C. Lai, *RSC Adv.*, 2018, **8**, 19341–19347.
27 A. J. Boydston, L. Bondarenko, I. Dix, T. J. R. Weakley, H. Hopf and M. M. Haley, *Angew. Chem., Int. Ed.*, 2001, **40**, 2986–2989.
28 J. L. Zafra, A. M. Ontoria, P. M. Burrezo, M. Pena-Alvarez, M. Samoc, J. Szeremeta, F. J. Ramirez, M. D. Lovander, C. J. Droske, T. M. Pappenfus, L. Echegoyen, J. T. L. Navarrete, N. Martin and J. Casado, *J. Am. Chem. Soc.*, 2017, **139**, 3095–3105.
29 T. Ogoshi, K. Umeda, T. A. Yamagishi and Y. Nakamoto, *Chem. Commun.*, 2009, 4874–4876.
30 K. J. Weiland, N. Munch, W. Gschwind, D. Haussinger and M. Mayor, *Helv. Chim. Acta*, 2019, **102**(1), e1800205.
31 P. Li, T. J. Sisto, E. R. Darzi and R. Jasti, *Org. Lett.*, 2014, **16**, 182–185.
32 Y. Segawa, A. Fukazawa, S. Matsuura, H. Omachi, S. Yamaguchi, S. Irle and K. Itami, *Org. Biomol. Chem.*, 2012, **10**, 5979–5984.
33 Q. Huang, G. Zhuang, H. Jia, M. Qian, S. Cui, S. Yang and P. W. Du, *Angew. Chem., Int. Ed.*, 2019, **58**, 6244–6249.
34 Y. Morisaki and Y. Chujo, *Macromolecules*, 2003, **36**, 9319–9324.
35 Y. Morisaki and Y. Chujo, *Angew. Chem., Int. Ed.*, 2006, **45**, 6430–6437.
36 J. W. Hong, H. Y. Woo, B. Liu and G. C. Bazan, *J. Am. Chem. Soc.*, 2005, **127**, 7435–7443.
37 J. Zyss, I. Ledoux, S. Volkov, V. Chernyak, S. Mukamel, G. P. Bartholomew and G. C. Bazan, *J. Am. Chem. Soc.*, 2000, **122**, 11956–11962.
38 H. Y. Woo, D. Korystov, Y. Jin and H. Suh, *Bull. Korean Chem. Soc.*, 2007, **28**, 2253–2260.
39 T. Miyazaki, M. Shibahara, J. Fujishige, M. Watanabe, K. Goto and T. Shinmyozu, *J. Org. Chem.*, 2014, **79**, 11440–11453.
40 G. P. Bartholomew and G. C. Bazan, *J. Am. Chem. Soc.*, 2002, **124**, 5183–5196.
41 F. Zhang, R. Zhang, X. Liang, K. Guo, Z. Han, X. Lu, J. Xie, J. Li, D. Li and X. Tian, *Dyes Pigm.*, 2018, **155**, 225–232.
42 P. C. Shen, Z. Y. Zhuang, X. F. Jiang, J. S. Li, S. N. Yao, Z. J. Zhao and B. Tang, *J. Phys. Chem. Lett.*, 2019, **10**, 2648–2656.
43 C. Y. Yu, C. H. Sie and C. Y. Yang, *New J. Chem.*, 2014, **38**, 5003–5008.
44 L. Guyard, C. Dumas, F. Miomandre, R. Pansu, R. Renault-Meallet and P. Audebert, *New J. Chem.*, 2003, **27**, 1000–1006.
45 W. D. Luke and A. Streitwieser, *J. Am. Chem. Soc.*, 1981, **103**, 3241–3243.
46 G. Yang, X. W. Han, W. P. Zhang, X. M. Liu, P. Y. Yang, Y. G. Zhou and X. H. Bao, *J. Phys. Chem. B*, 2005, **109**, 18690–18698.
47 B. M. Beser, M. Arik and Y. Onganer, *Luminescence*, 2019, **34**, 415–425.
48 B. Valeur, *Digital Encycl. Appl. Phys.*, 2003, 477–531.
49 T. Ogoshi, R. Shiga, M. Hashizume and T. Yamagishi, *Chem. Commun.*, 2011, **47**, 6927–6929.
50 M. J. Frisch, G. W. Trucks, H. B. Schlegel and G. E. Scuseria, *et al.*, *Gaussian 09 Software Revision A.02*, Gaussian Inc., Wallingford, 2009.

